Synergistic antitumor effects of 5-FU and Apatinib on papillary thyroid cancer in vitro and in vivo

Keywords
angiogenesis, 5-FU, papillary thyroid cancer, drug combination, Apatinib, TPC-1

Abstract
Introduction
Papillary thyroid carcinoma (PTC) is the most common type of thyroid malignancy with increased incidence rapidly occurring in most countries. The study aimed to investigate the antitumor effects of the combination of 5-FU and Apatinib on PTC.

Material and methods
TPC-1 and SW579 cells were treated with 5-FU, Apatinib, or a combination of 5-FU and Apatinib. Cell viability was assessed by the CCK-8 assay. Edu staining and colony formation were used to evaluate the cell proliferation ability. Flow cytometry was used to analyze the cell apoptosis. Wound healing and the Transwell assay were conducted to analyze cell migration and invasion. The angiogenesis of TPC-1 and SW579 cells was assessed by conducting the tube formation assay. Xenograft tumor models were established by injecting TPC-1 cells into nude mice. Expressions of CD31, VEGFA, and VEGFR2 were determined using immunofluorescence and Western blotting.

Results
Compared with 5-FU or Apatinib treatment alone, the combination of 5-FU and Apatinib produced stronger suppressive effects on cell proliferation, migration, invasion, and angiogenesis. An in vivo experiment showed that the combination of 5-FU and Apatinib strongly suppressed tumor growth. The combination of 5-FU and Apatinib remarkably suppressed expressions of CD31, VEGFA, and VEGFR2, associated with angiogenesis.

Conclusions
Our data demonstrated that 5-FU combined with Apatinib therapy obtained synergistic antitumor effects in PTC, compared with either 5-FU or Apatinib alone by down-regulating VEGFA/VEGFR2 signaling pathways.

Explanation letter
Review 1:
The authors made some useful corrections, especially in discussion part. But there is a logical mistake. The discussion part starts with side effects of the drugs. This knowledge should be discussed in the middle of the discussion part, so the discussion part needs rearrangement.
It is better to start discussion with the paragraph which starts as “We provided for the first time evidence that the combination of 5-FU (50 mg/kg) and Apatinib (200 mg/kg) could produce stronger synergistic effects in suppressing TPC-1 cell proliferation, migration, and invasion, compared with either 5-FU or Apatinib treatment alone”.

Respond: Thanks for your suggestion. The contents about the side effects of the drugs have been moved to the middle of the discussion section. And the disccssion starts as“We provided for the first time evidence that the combination of 5-FU (50 mg/kg) and Apatinib (200 mg/kg) could produce stronger synergistic effects in suppressing TPC-1 cell proliferation, migration, and invasion, compared with either 5-FU or Apatinib treatment alone”.

Explanation letter.docx

Synergistic antitumor effects of 5-FU and Apatinib on papillary thyroid cancer *in vitro* and *in vivo*

Min Meng, Xin Ye*, Xia Yang, Guanghui Huang, Zhigang Wei, Yang Ni, Wenhong Li, Xiaoying Han, Jiao Wang

Department of Oncology, Shandong Provincial Hospital Affiliated to Shandong First Medical University, Jinan, Shandong 250021, China.

Running title: Synergistic effects of 5-FU and Apatinib in PTC

***Corresponding author:**

Dr. Xin Ye

E-mail Address: Department of Oncology, Shandong Provincial Hospital Affiliated to Shandong First Medical University, No. 324 Jingwuweiqi Road, Jinan, Shandong 250021, China.

Phone: +86 0531-68773171,

Fax: +86 0531-68773172,

E-mail: yexintaian2014@163.com.

Abstract:

Introduction: Papillary thyroid carcinoma (PTC) is the most common type of thyroid malignancy with increased incidence rapidly occurring in most countries. The study aimed to investigate the antitumor effects of the combination of 5-FU and Apatinib on PTC.

Material and methods: TPC-1 and SW579 cells were treated with 5-FU, Apatinib, or a combination of 5-FU and Apatinib. Cell viability was assessed by the CCK-8 assay. Edu staining and colony formation were used to evaluate the cell proliferation ability. Flow cytometry was used to analyze the cell apoptosis. Wound healing and the Transwell assay were conducted to analyze cell migration and invasion. The angiogenesis of TPC-1 and SW579 cells was assessed by conducting the tube formation assay. Xenograft tumor models were established by injecting TPC-1 cells into nude mice. Expressions of CD31, VEGFA, and VEGFR2 were determined using immunofluorescence and Western blotting.

Results: Compared with 5-FU or Apatinib treatment alone, the combination of 5-FU and Apatinib produced stronger suppressive effects on cell proliferation, migration, invasion, and angiogenesis. An *in vivo* experiment showed that the combination of 5-FU and Apatinib strongly suppressed tumor growth. The combination of 5-FU and Apatinib remarkably suppressed expressions of CD31, VEGFA, and VEGFR2, associated with angiogenesis.

Conclusion: Our data demonstrated that 5-FU combined with Apatinib therapy obtained synergistic antitumor effects in PTC, compared with either 5-FU or Apatinib alone by down-regulating VEGFA/VEGFR2 signaling pathways.

Keywords: papillary thyroid cancer, TPC-1, 5-FU, Apatinib, drug combination, angiogenesis

Introduction

Papillary thyroid carcinoma (PTC) originating from thyroid epithelial cells is the most prevalent subtype of thyroid cancers accounting for approximately 80% of cases [1]. Despite that good clinical outcomes have been achieved by thyroidectomy, supplemented with postoperative radiotherapy and chemotherapy, the prognosis of PTC patients still remains unfavorable, mainly due to recurrence and metastasis[2, 3]. Therefore, understanding the molecular mechanism is helpful for developing therapeutic agents/drugs against PTC.

Angiogenesis is the process of new blood vessel formation from existing vessels and includes vascular endothelial cell migration and new tube formation[4] . Accumulating evidences have verified that dysregulation of angiogenesis is a critical hallmark in tumor formation and progression[5, 6]. Multiple growth factors have been reported to promote tumor angiogenic processes, of which vascular endothelial growth factor A (VEGFA), VEGF, and its primary receptors (VEGFR1, VEGFR2, and VEGFR-3) are the most critical drivers of angiogenesis[7-9]. As demonstrated by Lennard et al [10], VEGFA is overexpressed in PTC and its expression is associated with the incidence of metastasis. Thus, anti-angiogenic drugs have tremendous clinical value for advanced PTC failure from multi-lines of therapies.

5-FU has been widely used among patients with breast cancer [11], colorectal carcinoma [12], and pancreatic carcinoma [13]. However, severe side effects and drug resistance cannot be avoided and this situation limited for further clinical application [14]. Apatinib, a highly selected tyrosine kinase inhibitor targeting VEGFR-2, can effectively inhibit the proliferation, migration, and neovascularization of endothelial cells [15], and was approved for the second-line treatment of advanced gastric cancer in 2014 by China[16]. Moreover, Apatinib exerts potential benefits in advanced non-small cell lung cancer patients after multi-line therapies [17, 18]. Although usage of 5-FU or Apatinib monotherapy has shown efficacy for tumor therapy, more drug toxicity usually occurs with a higher dosage. The combination of 5-FU and Apatinib obtains better

therapeutic effects in advanced gastric cancer, which was reported by Xu et al [19]. Interestingly, Apatinib has been shown to inhibit angiogenesis in anaplastic thyroid cancer [20] and is a new option for the treatment of advanced medullary thyroid carcinoma[21]. However, whether the combination of 5-FU and Apatinib has a synergistic antitumor effect on PTC cells has not been previously determined.

In the present study, we explored the effects of 5-FU combined with Apatinib on TPC-1 cell proliferation, migration, invasion, and angiogenesis, compared with either 5-FU or Apatinib treatment alone. Furthermore, we constructed a xenograft tumor model to further evaluate the antitumor effects of 5-FU and Apatinib *in vivo*. The mechanism of the regulatory role of 5-FU and Apatinib on the molecules associated with angiogenesis was further explored *in vitro* and *in vivo*.

Materials and Methods

Cell culture and treatments.

Human TPC-1 and SW579 cells were purchased from the American Type Culture Collection and cultured in DMEM supplemented with 10% FBS (Thermo Fisher Scientific, Waltham, MA, USA) and 1% v/v penicillin/streptomycin (Solarbio, Beijing, China) in a humidified atmosphere containing 5% CO_2 at 37 °C. For the *in vitro* experiments, 5-FU and Apatinib were provided by Hengrui Medicine Co. Ltd. (Jiangsu, China) and dissolved in DMSO Sigma-Aldrich (StLouis, MO) before use. Then, TPC-1 cells were treated with 5-FU (70 μM), Apatinib (10 μM), or the combination of 5-FU and Apatinib for 48 h. The coefficient of drug interaction (CDI) was calculated as follows: $CDI = AB/(A \times B)$. The CDI calculations were carried out on SW579 and TPC-1 (**Supplementary table1, table2**).

Cell viability assay.

For the cell viability assay, TPC-1 and SW579 cells were seeded into 96-well plates in triplicate at a density of 4×10^3 cells per well and then subjected to drug treatment as indicated above. After 48 h, cells in each well were incubated with 10 μL CCK-8 reagent solution (Dojindo, Kumamoto, Japan) for 2 h at 37 °C. Subsequently, the optical

density (OD) was measured using a microplate reader at a wavelength of 450 nm.

EdU staining assay.

Cell proliferation was assessed by Cell-Light EdU Apollo 488 in the *in vitro* Imaging Kit (RiboBio, Guangzhou, China) according to the manufacturer's protocol. TPC-1 cells and SW579 cells (1×10^5 cell) were fixed with cold 4% formaldehyde for 30 min at room temperature, stained with 50 μM EdU labeling medium, and reacted with 150 μl of 1 × Apollo® for 30 min in the dark. DAPI was used to stain the cell nuclei for 30 min at room temperature. The red signal (Edu-positive cells) was detected under a fluorescent microscope (Olympus, Japan) at a magnification of ×200.

Colony formation assay.

TPC-1 cells and SW579 cells were subjected to analysis of the capacity of colony formation. Cells at a density of 500 cells per well were seeded into six-well plates and cultured for two weeks. The naturally formed colonies were fixed with 70% ethanol and stained with 0.1% crystal violet. The number of colonies (at least 50 cells per colony) was counted under a light microscope.

Flow cytometry analysis.

Cell apoptosis analysis was conducted using an Annexin V-FITC/PI Apoptosis Detection Kit (KeyGEN BioTECH, Jiangsu, China). TPC-1 and SW579 cells (1×10^5 cells) were washed twice in cold PBS and re-suspended in Annexin V-binding buffer. Then, cells were incubated with 5 μL of Annexin V-FITC and 5 μL of PI solution for 15 min at room temperature in the dark. After being treated with 400 μL 1×binding buffer, apoptotic cells were analyzed using a flow cytometer (BD Biosciences, San Jose, CA, USA).

Wound healing assay.

Cell migration was evaluated using a wound healing assay. TPC-1 cells and SW579 cells (5×10^6 cells) at a density of 2×10^5 cells per well were plated in six-well plates and a scratch wound was created with a 200-μl sterile pipette tip. Then the cells were cultured in serum-free medium for 48 h. Relative wound closure was estimated by

recording the wounds at the same position with a light microscope at 0 h and 48 h in five randomly selected fields.

Transwell invasion assay.

Cell invasion was evaluated with Transwell chambers (Corning, Lowell, MA, USA) coated with Matrigel (BD Bioscience, USA) in accordance with the manufacturer's instructions. TPC-1 cells and SW579 cells (5×10^4 cells) were suspended in 200μL serum-free medium and seeded onto the upper chambers and the medium containing 10% FBS was added to the lower chambers as a chemoattractant. After being cultured for 48 h, the invasive cells that migrated to the lower surface were fixed with 20% methanol, stained with 0.1% crystal violet, and counted under a microscope (Olympus, Japan) at 200× magnification.

Tube formation assay.

The angiogenesis of TPC-1 cells and SW579 cells was assessed by conducting a tube formation assay according to the protocol previously described [22]. TPC-1 cells and SW579 cells at a density of 1×10^5 cells/well were cultured in a 24-well plate pre-coated with 60 μL of Matrigel (BD Biosciences). After 8 h of incubation, cells were fixed with 4% paraformaldehyde and the capillary-like structures were viewed using an inverted microscope (Nikon, Tokyo, Japan).

Immunofluorescence.

TPC-1 cells and SW579 cells (5×10^4 cells) were washed twice with PBS, fixed with 4% paraformaldehyde for 10 min at room temperature, and permeabilized with 0.5%Triton X-100 for 5 min. After being blocked in PBS containing 3% bovine serum albumin for 1 h, the cells were incubated with primary antibodies against CD31, VEGFA, and VEGFR2 overnight at 4°C. Subsequently, cells were incubated with Alexa Fluor 488-conjugated or Alexa Fluor 647-conjugated secondary antibodies (Abcam, Cambridge, MA, USA) at room temperature for 1.5 h. The cell nuclei were stained with DAPI. After being washed twice with PBS, the stained images (magnification, ×200) were visualized by a Zeiss LSM700 confocal microscope (Zeiss AG).

Xenograft tumor model.

Male BALB/c nude mice (3-4-week-old, 19–21g) were purchased from Guangdong Experimental Animal Center (Guangdong, China) and kept under specific pathogen-free conditions. Xenograft models were established by subcutaneous injections of approximately 2×10^6 TPC-1 cells into the same side armpit of each nude mouse. Then, the mice were treated with Apatinib (200 mg/kg), 5-FU (50 mg/kg), 5-FU plus Apatinib, or PBS once daily by oral gavage for four weeks, and were accordingly divided into four groups with five mice per group. During this time, the tumor volume was monitored and calculated as Volume = (length × width^2)/2. At day 30, the animals were sacrificed by cervical decapitation and tumor tissues were removed for further analysis. All animal procedures were approved by the Experimental Animal Ethics Committee of Shandong Provincial Hospital Affiliated to Shandong First Medical University and in accordance with institutional animal care and use committee guidelines.

Quantitative real time PCR.

Total RNA was extracted with Trizol reagent (Invitrogen, CA, USA) and cDNA was synthesized with a Reverse Transcription Kit (Takara Inc, USA) according to the manufacturer's instructions. Real-time PCR (RT-PCR) was performed on a Roche LightCycler480 Real-Time PCR System using the SYBR Green PCR kit (Takara, Dalian, China) with the following primer sequences: CD31-forward: 5'-AACAGTGTTGACATGAAGAGCC-3' and CD31-reverse: 5'-TGTAAAACAGCACGTCATCCTT-3'; VEGFA-forward: 5'-AGGGCAGAATCATCACGAAGT-3' and VEGFA-reverse: 5'-AGGGTCTCGATTGGATGGCA-3'; VEGFR2-forward: 5'-GGCCCAATAATCAGAGTGGCA-3' and VEGFR2-reverse: 5'-CCAGTGTCATTTCCGATCACTTT-3'; GAPDH-forward: 5'-TGTTCGTCATGGGTGTGAAC-3' and GAPDH-reverse: 5'-ATGGCATGGACTGTGGTCAT-3'. The relative gene expression level was calculated by the $2^{-\Delta\Delta CT}$ method with GAPDH as the endogenous control.

Western blot.

Total protein samples were extracted using RIPA lysis buffer with protease inhibitors (Beyotime, Haimen, China). Equal amounts of protein were separated on 10% SDS-PAGE gel and electro-transferred to PVDF membranes. The membranes were blocked with 5% non-fat milk for 2 h and probed with primary antibodies against CD31, VEGFA, VEGFR2, and GAPDH overnight at 4°C followed by the HRP-conjugated secondary antibody. After being twice washed with PBS, the protein signals were detected using the enhanced chemiluminescent (ECL) detection system (Amersham, GE Healthcare, Chicago, IL, USA). GAPDH served as the loading control.

Immuno-histochemistry

Tissues were fixed in 4% paraformaldehyde and embedded in paraffin afterwards. Then embedded tissues were cut into slices (4 μm) and followed by dehydration and dewaxing. Subsequently, slices were performed an antigen repairment, peroxidase deactivation and blocking. Afterwards, slices were incubated with primary antibody and secondary antibody and then developed using DAB staining kit. Finally, slices were re-stained using Harris and sealed by neutral resins for observation under a microscope.

Statistical analysis.

All experiments were performed independently at least three times and quantitative data are expressed as the mean ± standard deviation (SD). Statistical analysis was performed using GraphPad Prism software (GraphPad Software Inc., La Jolla, CA) with one-way ANOVA analysis, followed by Tukey's test. The values of p less than 0.05 were considered to be statistically significant.

Results

The effects of 5-FU, Apatinib, or their combination on cell proliferation and apoptosis in TPC cells and SW579 cells.

To evaluate the synergistic effect of 5-FU and Apatinib on cell proliferation, TPC-1 cells were subjected to 5-FU, Apatinib, or 5-FU + Apatinib treatment. IC50 of TPC cells

and SW579 cells to 5-FU was measured. As shown in **Figure 1A and 2A**, IC50 of TPC and SW579 was 100.95 μM and 103.11 μM. CCK8 assay showed that both 5-FU and Apatinib treatments significantly reduced cell viability, which was further enhanced by the combination of 5-FU and Apatinib (Figure 1B and Figure 2B). It was demonstrated that 5-FU + Apatinib treatment further promoted the decreased cell proliferation induced by either 5-FU or Apatinib treatment, as reflected by less Edu-positive cells (**Figure 1C and Figure 2C**) and colonies (**Figure 1D and Figure 2D**). Annexin V/PI apoptosis analysis showed that 5-FU had a synergistic effect on Apatinib that significantly induced apoptosis in TPC-1 cells (**Figure 1E and Figure 2E**). These results suggest that both 5-FU and Apatinib not only induced apoptosis of TPC-1 and SW579 cells but also exhibited a strong synergistic effect when combined (see Supplemented Table 1).

The effects of 5-FU, Apatinib, or their combination on migration, invasion, and angiogenesis in TPC cells and and SW579 cells.

Next, the synergistic effect of 5-FU and Apatinib was assessed on migration, invasion, and angiogenesis in TPC-1 and SW579 cells. The results from the wound healing assay showed that continuous rapid movement was found in the control group compared with cells treated with 5-FU, Apatinib, or their combination (**Figure 3A and Figure 4A**). Quantitative analysis further indicated that the wounded areas in the control group were significantly decreased compared with 5-FU or Apatinib and further reduced compared with the combination of 5-FU and Apatinib (**Figure 3C and Figure 4C**), which indicated a strong synergistic effect in attenuating cell migration. In addition, the Transwell assay demonstrated that either 5-FU or Apatinib treatment remarkably reduced the number of invasive cells, which was further enhanced by the combination of 5-FU and Apatinib (**Figure 3B, 3D, Figure 4B, 4D**). Furthermore, a strong synergistic effect of 5-FU and Apatinib on decreased tube length was found compared with 5-FU or Apatinib treatment alone (**Figure 5**) (see Supplemented Table 1).

The effects of 5-FU, Apatinib, or their combination on the molecules associated with angiogenesis.

To explore the mechanism underlying 5-FU and Apatinib suppression of angiogenesis, we analyzed the protein expression of growth factors in angiogenesis using immunofluorescence. As depicted in **Figure 6 and Figure 7**, the micro-vessel density marker differentiation 31 (CD31), vascular endothelial growth factor A (VEGFA), and epidermal growth factor receptor (EGFR) were obviously down-regulated in TPC-1 cells after either 5-FU or Apatinib treatment and further reduced after the combination of 5-FU and Apatinib. Additionally, 5-FU or Apatinib treatment alone decreased expression of VEGFR2, an important VEGF receptor and their combination produced a stronger suppressive effect on VEGFR2 expression (see Supplemented Table 1).

The effects of 5-FU, Apatinib, or their combination on tumor growth and angiogenesis in vivo.

Subsequently, to further explore the effect of 5-FU and Apatinib on tumor growth *in vivo*, xenograft tumor models were established by injecting TPC-1 cells into nude mice, followed by administration of Apatinib, 5-FU, 5-FU plus Apatinib, or PBS by oral gavage. After 30 days, nude mice in the control group developed visible tumors, while relatively smaller tumors were observed in Apatinib and 5-FU groups and the smallest tumors were in the 5-FU plus Apatinib group (**Figure 8A**). Every 3 days, the subcutaneous tumors were measured and data showed that the combination of Apatinib and 5-FU remarkably suppressed the tumor volume at consecutive days (**Figure 8B**). Consistent with the *in vitro* study, quantitative real time PCR (**Figure 8C**) and Western blot analysis (**Figure 8D**) further demonstrated that either 5-FU or Apatinib suppressed expressions of CD31, VEGFA, andVEGFR2, associated with angiogenesis. Finally, Caspase 3 was enhanced by 5-FU or Apatinib, and expression was promoted in tissues of 5-FU and Apatinib group (**Figure 8E**). Besides, expression of Ki67 in tissues was

detected by using IHC. Results in Figure 8F showed that Ki67 expression was suppressed by 5-FU or Apatinib, and inhibitive effect was strengthened when 5-FU and Apatinib was administrated at the same time (**Figure 8F**) (see Supplemented Table 1).

Discussion

We provided for the first time evidence that the combination of 5-FU (50 mg/kg) and Apatinib (200 mg/kg) could produce stronger synergistic effects in suppressing TPC-1 cell proliferation, migration, and invasion, compared with either 5-FU or Apatinib treatment alone. Consistent with our data, Xu et al [19] showed that the combination of 5-Fu and Apatinib enhanced the chemosensitivity of a gastric cancer cell line and it was more effective for gastric cancer treatment than 5-Fu alone. Feng et al [23] reported that the combination therapy of Apatinib and 5-FU was effective and well tolerated in the treatment of gastric cancer *in vivo* and *in vitro*.

Apatinib, an anti-angiogenic agent, exerting cytostatic activity rather than cytotoxicity, showed modest survival benefits. Some studies have confirmed that the combination of Apatinib and cytotoxic drugs increased the antitumor effect and alleviated side effects[24-26]. Previous reports indicated that 50 to 200mg/kg/day apatinib was necessary to achieve anticancer effects in different mouse models [24, 27, 28].

Like other chemotherapeutic drugs, 5-FU has been reported to exhibit systemic toxicities, including, likely hepatotoxicity and nephrotoxicity[29]. 5-FU is catabolized into dihydrouracil in the liver which is cleaved into urea, ammonia, and carbon dioxide, thus causing nephrotoxicity [29, 30]. 5-FU is eliminated from the body via hepatic metabolism and toxic intermediates produced during the metabolism of 5-FU are majorly responsible for hepatotoxicity[31]. Generally, a high dose of 5-fluorouracil (200 or 400 mg/kg) was used to build the mouse model of chemotherapy [30, 32].

A combination of tegafur, gimeracil, and oteracil potassium, named S-1, has been widely used in treatment of multiple cancers[33]. S-1 is converted into fluorouracil after

internalization into cells, and S-1 shares similar anticancer properties as intravenous 5-Fu[34].The clinical study of 84 patients with advanced gastric cancer showed that the progression free survival (PFS) of patients was overtly longer in the Apatinib + S-1(a fluorouracil drug) group than that in S-1 group[35]. Capecitabine is a novel drug that can be well absorbed after oral administration, and converted into 5-FU by thymidine phosphorylase in tumor tissues[36]. Capecitabine has been confirmed to replace 5-FU for the gastrointestinal chemoradiation therapy[37]. The oral combination of apatinib and S-1/capecitabine achieved satisfactory disease control in esophageal squamous cell carcinoma patients with residual disease after definitive concurrent chemoradiotherapy[33]. Zhao et al. [38]reported that the combination therapy of apatinib and S-1 was effective in the treatment of advanced squamous cell carcinoma patients. The combination of apatinib and capecitabine regimen can achieve a better efficacy than capecitabine alone as the third-line treatment for advanced triple-negative breast cancer[39].In the present study, we investigated the synergistic effect of Apatinib and 5-FU in TPC-1 and SW579 cells.

What is more, we found a strong suppressive effect of 5-FU and Apatinib on angiogenesis, as reflected by decreased tube length, compared with 5-FU or Apatinib treatment alone. The growth of tumor cells mainly depends on the oxygen and nutrients supplied by tumor angiogenesis [40]. Tumor angiogenesis requires interactions among tumor cells and mesenchymal cells through growth factors and their corresponding receptors[41]. VEGF is an important signaling pathway involved in neovascularization[42]. VEGF can be activated when combined with its receptor (VEGFRs) and activated VEGF promotes vascular cell proliferation to develop a new blood supply, leading to tumor growth and metastasis[43]. Among the VEGFRs, VEGFR2 is considered to be the most relevant factor associated with tumor angiogenesis[44]. Related studies indicated that Apatinib can inhibit the VEGF signaling pathway by destroying the interaction between VEGF-A and VEGFR-2[45, 46]. In line with these facts, our data showed that the combination of 5-FU and Apatinib

strongly suppressed expressions of CD31, VEGFA, and VEGFR2, associated with angiogenesis *in vitro* and *in vivo*. Thus, targeting VEGF might be a promising therapeutic strategy for PTC pathogenesis, indicating that it is feasible to combine apatinib with other chemotherapeutic agents to yield a synergistic effect in the treatment of PTC.

Conclusion

In conclusion, our preliminary study demonstrated that 5-FU combined with Apatinib therapy obtained synergistic antitumor effects in PTC cells, compared with either 5-FU or apatinib alone by suppressing cell proliferation, migration, invasion, and angiogenesis via down-regulating VEGFA/VEGFR2 signaling pathways (Figure 9). In the future, large-scale, prospective, randomized clinical studies are needed to validate and expand the findings of our study.

Funding Statement

This work was financially supported by National Natural Science Foundation of China (Grant number 30973673).

Conflicts of Interest

The authors declare that they have no conflict of interest.

References

1. Lang B H, Lo C Y, Chan W F, Lam A K, Wan K Y. Classical and follicular variant of papillary thyroid carcinoma: a comparative study on clinicopathologic features and long-term outcome. World J Surg 2006; 30: 752-8.
2. Asimakopoulos P, Nixon I J, Shaha A R. Differentiated and Medullary Thyroid Cancer: Surgical Management of Cervical Lymph Nodes. Clin Oncol (R Coll Radiol) 2017; 29: 283-289.
3. Wang L Y, Ganly I. Nodal metastases in thyroid cancer: prognostic implications and management. Future Oncol 2016; 12: 981-94.
4. Tonnesen M G, Feng X, Clark R A. Angiogenesis in wound healing. J Investig Dermatol Symp Proc 2000; 5: 40-6.
5. Kuol N, Stojanovska L, Apostolopoulos V, Nurgali K. Role of the Nervous System in Tumor Angiogenesis. Cancer Microenviron 2018; 11: 1-11.

367 6. Ronca R, Benkheil M, Mitola S, Struyf S, Liekens S. Tumor angiogenesis revisited: Regulators and
368 clinical implications. Med Res Rev 2017; 37: 1231-1274.
369 7. Yancopoulos G D, Davis S, Gale N W, Rudge J S, Wiegand S J, Holash J. Vascular-specific growth
370 factors and blood vessel formation. Nature 2000; 407: 242-8.
371 8. Risau W. Mechanisms of angiogenesis. Nature 1997; 386: 671-4.
372 9. Lin J X, Weng X F, Xie X S, et al. CDK5RAP3 inhibits angiogenesis in gastric neuroendocrine
373 carcinoma by modulating AKT/HIF-1alpha/VEGFA signaling. Cancer Cell Int 2019; 19: 282.
374 10. Lennard C M, Patel A, Wilson J, et al. Intensity of vascular endothelial growth factor expression
375 is associated with increased risk of recurrence and decreased disease-free survival in papillary
376 thyroid cancer. Surgery 2001; 129: 552-8.
377 11. Zhan Y, Ma W, Zhang Y, et al. DNA-Based Nanomedicine with Targeting and Enhancement of
378 Therapeutic Efficacy of Breast Cancer Cells. ACS Appl Mater Interfaces 2019; 11: 15354-15365.
379 12. Wang W, Guo W, Li L, et al. Andrographolide reversed 5-FU resistance in human colorectal
380 cancer by elevating BAX expression. Biochem Pharmacol 2016; 121: 8-17.
381 13. Ducreux M, Mitry E, Ould-Kaci M, et al. Randomized phase II study evaluating oxaliplatin alone,
382 oxaliplatin combined with infusional 5-FU, and infusional 5-FU alone in advanced pancreatic
383 carcinoma patients. Ann Oncol 2004; 15: 467-73.
384 14. An Z J, Li Y, Tan B B, et al. Up-regulation of KLF17 expression increases the sensitivity of gastric
385 cancer to 5-fluorouracil. Int J Immunopathol Pharmacol 2021; 35: 20587384211010925.
386 15. Zhang H. Apatinib for molecular targeted therapy in tumor. Drug Des Devel Ther 2015; 9: 6075-
387 81.
388 16. Roviello G, Ravelli A, Polom K, et al. Apatinib: A novel receptor tyrosine kinase inhibitor for the
389 treatment of gastric cancer. Cancer Lett 2016; 372: 187-91.
390 17. Xu J, Liu X, Yang S, Zhang X, Shi Y. Clinical response to apatinib monotherapy in advanced non-
391 small cell lung cancer. Asia Pac J Clin Oncol 2018; 14: 264-269.
392 18. Wu F, Zhang S, Gao G, Zhao J, Ren S, Zhou C. Successful treatment using apatinib with or
393 without docetaxel in heavily pretreated advanced non-squamous non-small cell lung cancer: A
394 case report and literature review. Cancer Biol Ther 2018; 19: 141-144.
395 19. Xu Z, Hu C, Chen S, et al. Apatinib enhances chemosensitivity of gastric cancer to paclitaxel and
396 5-fluorouracil. Cancer Manag Res 2019; 11: 4905-4915.
397 20. Jin Z, Cheng X, Feng H, et al. Apatinib Inhibits Angiogenesis Via Suppressing Akt/GSK3beta/ANG
398 Signaling Pathway in Anaplastic Thyroid Cancer. Cell Physiol Biochem 2017; 44: 1471-1484.
399 21. Chen K, Gao Y, Shi F, Cao G, Bao J. Apatinib-treated advanced medullary thyroid carcinoma: a
400 case report. Onco Targets Ther 2018; 11: 459-463.
401 22. Wang W, Wang H J, Wang B, et al. The Role of the Y Box Binding Protein 1 C-Terminal Domain in
402 Vascular Endothelial Cell Proliferation, Apoptosis, and Angiogenesis. DNA Cell Biol 2016; 35: 24-
403 32.
404 23. Feng J, Qin S. The synergistic effects of Apatinib combined with cytotoxic chemotherapeutic
405 agents on gastric cancer cells and in a fluorescence imaging gastric cancer xenograft model.
406 Onco Targets Ther 2018; 11: 3047-3057.
407 24. Feng S Q, Wang G J, Zhang J W, et al. Combined treatment with apatinib and docetaxel in A549
408 xenograft mice and its cellular pharmacokinetic basis. Acta Pharmacol Sin 2018; 39: 1670-1680.
409 25. Mi Y J, Liang Y J, Huang H B, et al. Apatinib (YN968D1) reverses multidrug resistance by

410 inhibiting the efflux function of multiple ATP-binding cassette transporters. Cancer Res 2010; 70:
411 7981-91.
412 26. Tong X Z, Wang F, Liang S, et al. Apatinib (YN968D1) enhances the efficacy of conventional
413 chemotherapeutical drugs in side population cells and ABCB1-overexpressing leukemia cells.
414 Biochem Pharmacol 2012; 83: 586-97.
415 27. Lin Y, Zhai E, Liao B, et al. Autocrine VEGF signaling promotes cell proliferation through a PLC-
416 dependent pathway and modulates Apatinib treatment efficacy in gastric cancer. Oncotarget
417 2017; 8: 11990-12002.
418 28. Tian S, Quan H, Xie C, et al. YN968D1 is a novel and selective inhibitor of vascular endothelial
419 growth factor receptor-2 tyrosine kinase with potent activity in vitro and in vivo. Cancer Sci
420 2011; 102: 1374-80.
421 29. Yousef H N, Aboelwafa H R. The potential protective role of taurine against 5-fluorouracil-
422 induced nephrotoxicity in adult male rats. Exp Toxicol Pathol 2017; 69: 265-274.
423 30. Gelen V, Şengül E, Yıldırım S, Senturk E, Tekin S, Kükürt A. The protective effects of hesperidin
424 and curcumin on 5-fluorouracil-induced nephrotoxicity in mice. Environ Sci Pollut Res Int 2021;
425 28: 47046-47055.
426 31. Tateishi T, Watanabe M, Nakura H, et al. Dihydropyrimidine dehydrogenase activity and
427 fluorouracil pharmacokinetics with liver damage induced by bile duct ligation in rats. Drug
428 Metab Dispos 1999; 27: 651-4.
429 32. Fukuno S, Nagai K, Yoshida S, Suzuki H, Konishi H. Taurine as a protective agent for 5-
430 fluorouracil-induced hepatic damage related to oxidative stress. Pharmazie 2016; 71: 530-532.
431 33. Chi D, Chen B, Guo S, et al. Oral maintenance therapy using apatinib combined with S-
432 1/capecitabine for esophageal squamous cell carcinoma with residual disease after definitive
433 chemoradiotherapy. Aging (Albany NY) 2021; 13: 8408-8420.
434 34. Boku N, Yamamoto S, Fukuda H, et al. Fluorouracil versus combination of irinotecan plus
435 cisplatin versus S-1 in metastatic gastric cancer: a randomised phase 3 study. Lancet Oncol 2009;
436 10: 1063-9.
437 35. Wu Q, Fu Y, Wen W, Xi T, Zhao G. Efficacy and prognosis analyses of apatinib combined with S-1
438 in third-line chemotherapy for advanced gastric cancer. J buon 2020; 25: 987-994.
439 36. Patel A, Pluim T, Helms A, Bauer A, Tuttle R M, Francis G L. Enzyme expression profiles suggest
440 the novel tumor-activated fluoropyrimidine carbamate capecitabine (Xeloda) might be effective
441 against papillary thyroid cancers of children and young adults. Cancer Chemother Pharmacol
442 2004; 53: 409-14.
443 37. Rich T. Capecitabine and radiation therapy for advanced gastrointestinal malignancies. Oncology
444 (Williston Park) 2002; 16: 27-30.
445 38. Zhao J, Lei J, Yu J, et al. Clinical efficacy and safety of apatinib combined with S-1 in advanced
446 esophageal squamous cell carcinoma. Invest New Drugs 2020; 38: 500-506.
447 39. Li Y H, Zhou Y, Wang Y W, et al. Comparison of apatinib and capecitabine (Xeloda) with
448 capecitabine (Xeloda) in advanced triple-negative breast cancer as third-line therapy: A
449 retrospective study. Medicine (Baltimore) 2018; 97: e12222.
450 40. Jayson G C, Kerbel R, Ellis L M, Harris A L. Antiangiogenic therapy in oncology: current status and
451 future directions. Lancet 2016; 388: 518-29.
452 41. Lin J, Cao S, Wang Y, et al. Long non-coding RNA UBE2CP3 enhances HCC cell secretion of VEGFA

453 and promotes angiogenesis by activating ERK1/2/HIF-1α/VEGFA signalling in hepatocellular
454 carcinoma. J Exp Clin Cancer Res 2018; 37: 113.
455 42. Ferrara N. VEGF and the quest for tumour angiogenesis factors. Nat Rev Cancer 2002; 2: 795-
456 803.
457 43. Zhao J, Zhang X, Gong C, Zhang J. Targeted therapy with apatinib in a patient with relapsed
458 small cell lung cancer: A case report and literature review. Medicine (Baltimore) 2017; 96:
459 e9259.
460 44. Koch S, Tugues S, Li X, Gualandi L, Claesson-Welsh L. Signal transduction by vascular endothelial
461 growth factor receptors. Biochem J 2011; 437: 169-83.
462 45. Fontanella C, Ongaro E, Bolzonello S, Guardascione M, Fasola G, Aprile G. Clinical advances in
463 the development of novel VEGFR2 inhibitors. Ann Transl Med 2014; 2: 123.
464 46. Liu K, Ren T, Huang Y, et al. Apatinib promotes autophagy and apoptosis through
465 VEGFR2/STAT3/BCL-2 signaling in osteosarcoma. Cell Death Dis 2017; 8: e3015.

466
467
468
469
470
471
472
473
474
475
476
477
478
479
480
481
482
483
484

Figure legends

Figure 1 The effects of 5-FU, Apatinib. or their combination on cell proliferation and apoptosis in TPC-1 cells. TPC-1 cells were subjected to 5-FU, Apatinib, or 5-FU + Apatinib treatment. (A) IC50 of TPC cells to 5-FU was detected. (B) Cell viability was determined in TPC-1 cells. (C) Edu-positive cells were detected with Edu staining. (D) Representative images of colonies are shown (left panel) and quantification of colonies (right panel) in TPC-1 cells. (E) Flow cytometry images (left panel) and quantification of apoptotic TPC-1 cells (right panel). Data are expressed as the mean ±standard deviation. *p< 0.05, **p< 0.01, ***p< 0.001, compared with the control; #p< 0.05, ##p< 0.01, compared with 5-FU or Apatinib

Figure 2 The effects of 5-FU, Apatinib. or their combination on cell proliferation and apoptosis in SW579 cells. SW579 cells were subjected to 5-FU, Apatinib, or 5-FU + Apatinib treatment. (A) IC50 of SW579 cells to 5-FU was detected. (B) Cell viability was determined in TPC-1 cells. (C) Edu-positive cells were detected with Edu staining. (D) Representative images of colonies are shown (left panel) and quantification of colonies (right panel) in SW579 cells. (E) Flow cytometry images (left panel) and quantification of apoptotic SW579 cells (right panel). Data are expressed as the mean ±standard deviation. *p< 0.05, **p< 0.01, compared with the control; #p< 0.05, ##p< 0.01, compared with 5-FU or Apatinib

Figure 3 The effects of 5-FU, Apatinib, or their combination on migration and invasion in TPC-1 cells. TPC-1 cells were subjected to 5-FU, Apatinib, or 5-FU + Apatinib treatment. (A) TPC-1 cells in monolayers were wounded and the remaining cell monolayers were incubated in the medium for 48 h. At the 0 h and 48 h, the wound areas were photographed under a fluorescent microscope. (C) The relative wound area

was calculated in TPC-1 cells. (B) Representative images of invasive cells are shown and (D) quantification of invasive cells was calculated. Data are expressed as the mean ±standard deviation. **p< 0.01, compared with the control; #p< 0.05, ##p<0.01, compared with 5-FU or Apatinib

Figure 4 The effects of 5-FU, Apatinib, or their combination on migration and invasion in SW579 cells. SW579 cells were subjected to 5-FU, Apatinib, or 5-FU + Apatinib treatment. (A) TPC-1 cells in monolayers were wounded and the remaining cell monolayers were incubated in the medium for 48 h. At the 0 h and 48 h, the wound areas were photographed under a fluorescent microscope. (C) The relative wound area was calculated in SW579 cells. (B) Representative images of invasive cells are shown and (D) quantification of invasive cells was calculated. Data are expressed as the mean ±standard deviation. **p< 0.01, compared with the control; #p< 0.05, compared with 5-FU or Apatinib

Figure 5 The effects of 5-FU, Apatinib, or their combination on angiogenesis in TPC cells and SW579 cells. TPC-1 cells (A) and SW579 cells (B) were subjected to 5-FU, Apatinib, or 5-FU + Apatinib treatment. TPC-1 cells were seeded on Matrigel for 8 h to observe tube formation. Representative photographs are shown.

Figure 6 The effects of 5-FU, Apatinib, or their combination on the molecules associated with angiogenesis. TPC-1 cells were subjected to 5-FU, Apatinib, or 5-FU + Apatinib treatment. Representative immunofluorescent images of CD31, VEGFA, andVEGFR2.

Figure 7 The effects of 5-FU, Apatinib, or their combination on the molecules associated with angiogenesis. SW579 cells were subjected to 5-FU, Apatinib, or 5-FU

+ Apatinib treatment. Representative immunofluorescent images of CD31, VEGFA, andVEGFR2.

Figure 8 The effects of 5-FU, Apatinib, or their combination on tumor growth and angiogenesis *in vivo*. Xenograft tumor models were established by injecting TPC-1 cells into nude mice, followed by administration of Apatinib, 5-FU, 5-FU plus Apatinib, or PBS by oral gavage. (A) Xenograft tumors were harvested on day 30. (B) Graph showing the growth curve of the tumor in nude mice. (C) Quantitative real time PCR and (D) Western blot analysis were performed to determine expressions of CD31, VEGFA, andVEGFR2. (E and F) Caspase 3 (E) and Ki67 (F) was detected using IFC. Data are expressed as the mean ±standard deviation. *$p < 0.05$, **$p < 0.01$, compared with the control; #$p < 0.05$, ##$p < 0.01$, compared with 5-FU or Apatinib

Figure 9 Graphical Abstract.

Supplementary tables

Table 1. Drug interaction was analyzed by calculating coefficient of drug interaction (CDI) in SW579 cell line

	5-FU	Apatinib	5-FU+Apaptinib	CDI
Apoptosis	2.75	2.67	3.93	0.54
Colony formation	0.31	0.51	0.03	0.16
Migration	0.58	0.66	0.38	0.99
Invasion	0.52	0.53	0.16	0.56

Note: CDI, Cofficient of drug interation

Supplementary tables

Table 2. Drug interaction was analyzed by calculating coefficient of drug interaction (CDI) in PTC-1 cell line

	5-FU	Apatinib	5-FU+Apaptinib	CDI
Apoptosis	2.18	2.59	3.42	0.60
Colony formation	0.62	0.72	0.31	0.70
Migration	0.56	0.73	0.39	0.95
Invasion	0.52	0.53	0.16	0.56

Note: CDI, Cofficient of drug interation

Figure 1B and Figure 2B

CCK8				
TPC-1	Control	5-FU	Apatinib	5-FU+Apatinib
Mean	1.02	0.72	0.78	0.44
SD	0.06	0.02	0.02	0.02
SW579	Control	5-FU	Apatinib	5-FU+Apatinib
Mean	1.17	0.72	0.88	0.37
SD	0.02	0.08	0.07	0.04

Figure 1D and Figure 2D

Colony number				
TPC-1	Control	5-FU	Apatinib	5-FU+Apatinib
Mean	63.33	41.00	48.00	20.67
SD	7.77	8.00	7.00	3.06
SW579	Control	5-FU	Apatinib	5-FU+Apatinib
Mean	38.33	12.00	19.67	1.00
SD	6.11	2.65	5.03	1.00

Figure 1E and Figure 2E

Apoptosis rate (%)				
TPC-1	Control	5-FU	Apatinib	5-FU+Apatinib
Mean	8.70	19.00	22.57	29.73
SD	1.74	1.50	2.25	4.12
SW579	Control	5-FU	Apatinib	5-FU+Apatinib
Mean	7.27	19.10	18.50	27.27
SD	0.76	1.81	4.19	2.55

Figure 3C and Figure 4C

Migration index (%)				
TPC-1	Control	5-FU	Apatinib	5-FU+Apatinib
Mean	72.85	60.92	49.17	30.77
SD	0.67	1.12	0.79	0.70
SW579	Control	5-FU	Apatinib	5-FU+Apatinib
Mean	70.13	40.80	46.31	26.65
SD	0.37	0.65	1.42	0.98

Figure 3D and Figure 4D

Invasion cells per field				
TPC-1	Control	5-FU	Apatinib	5-FU+Apatinib
Mean	60.67	30.67	29.00	11.00
SD	3.51	2.52	2.65	1.00
SW579	Control	5-FU	Apatinib	5-FU+Apatinib
Mean	106.33	55.67	58.00	15.33
SD	6.11	6.03	7.21	1.53

Figure 8B

Tumor volume(mm3)		Control	5-FU	Apatinib	5-FU+Apatinib
0d	Mean	82.67	82.45	83.18	82.42
	SD	28.47	18.38	11.75	17.06
5d	Mean	141.25	98.39	140.21	93.76
	SD	53.64	16.07	20.92	23.31
10d	Mean	214.31	113.26	181.21	108.14
	SD	110.75	17.73	33.00	28.39

15d	Mean	338.94	137.97	232.29	122.40
	SD	181.80	24.31	54.37	31.07
20d	Mean	527.81	161.27	291.68	133.21
	SD	223.03	31.90	76.02	30.13
25d	Mean	849.87	222.99	436.73	149.12
	SD	342.77	37.03	91.22	37.21
30d	Mean	1275.35	310.60	656.32	181.00
	SD	440.45	65.02	147.91	39.82

Figure 8C

Relative expression of mRNA		Control	5-FU	Apatinib	5-FU+Apatinib
CD31	Mean	1.05	1.21	1.30	1.03
	SD	0.11	0.13	0.20	0.02
VEGFA	Mean	0.89	0.58	0.30	0.16
	SD	0.14	0.08	0.05	0.00
VEGFR2	Mean	1.13	1.30	1.32	1.22
	SD	0.12	0.17	0.22	0.09

Figure 8D

Relative expression of proteins		Control	5-FU	Apatinib	5-FU+Apatinib
CD31	Mean	0.92	0.75	0.68	0.63
	SD	0.02	0.04	0.06	0.03
VEGFR2	Mean	0.81	0.69	0.75	0.81
	SD	0.07	0.04	0.02	0.03
VEGFA	Mean	0.88	0.43	0.45	0.38
	SD	0.03	0.03	0.05	0.05
EGFR	Mean	1.54	1.59	1.55	1.65
	SD	0.07	0.05	0.04	0.04

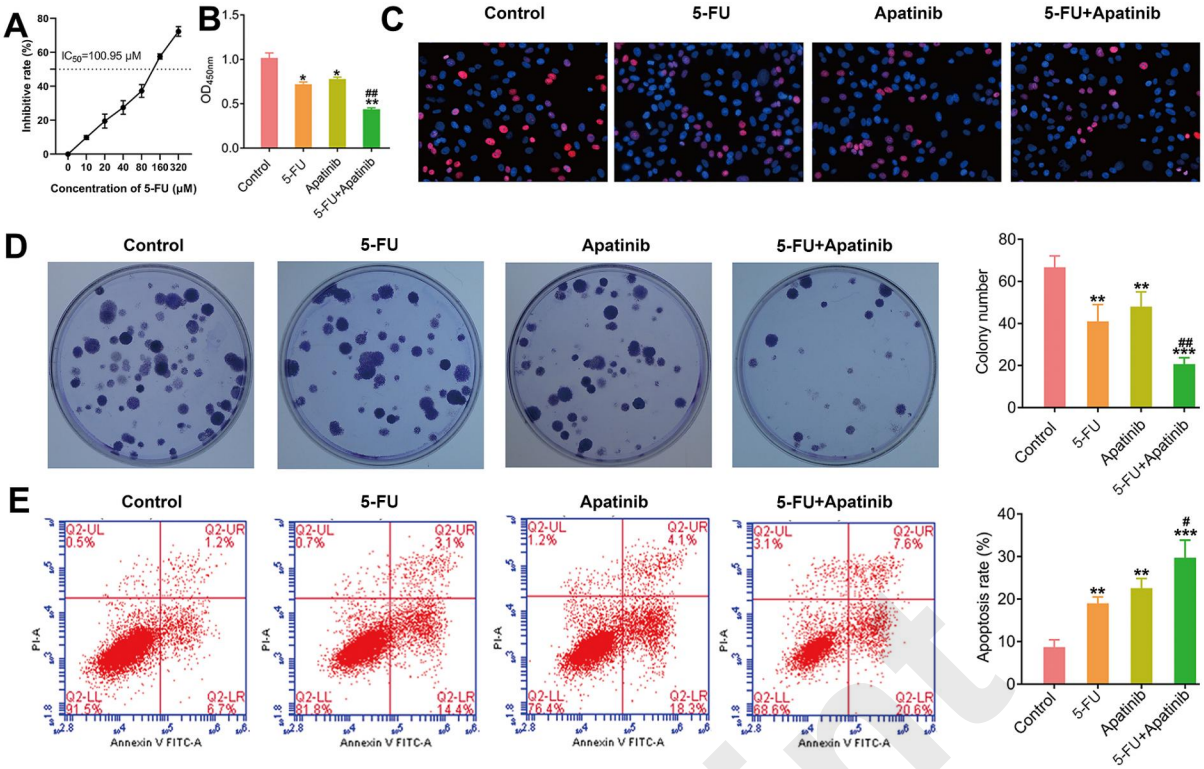
A
Inhibitive rate (%)
IC50=100.95 μM
Concentration of 5-FU (μM)
B
OD450nm
Control
5-FU
Apatinib
5-FU+Apatinib
C
Control
5-FU
Apatinib
5-FU+Apatinib
D
Control
5-FU
Apatinib
5-FU+Apatinib
Colony number
E
Control
5-FU
Apatinib
5-FU+Apatinib
Q2-UL
Q2-UR
Q2-LL
Q2-LR
PI-A
Annexin V FITC-A
Apoptosis rate (%)

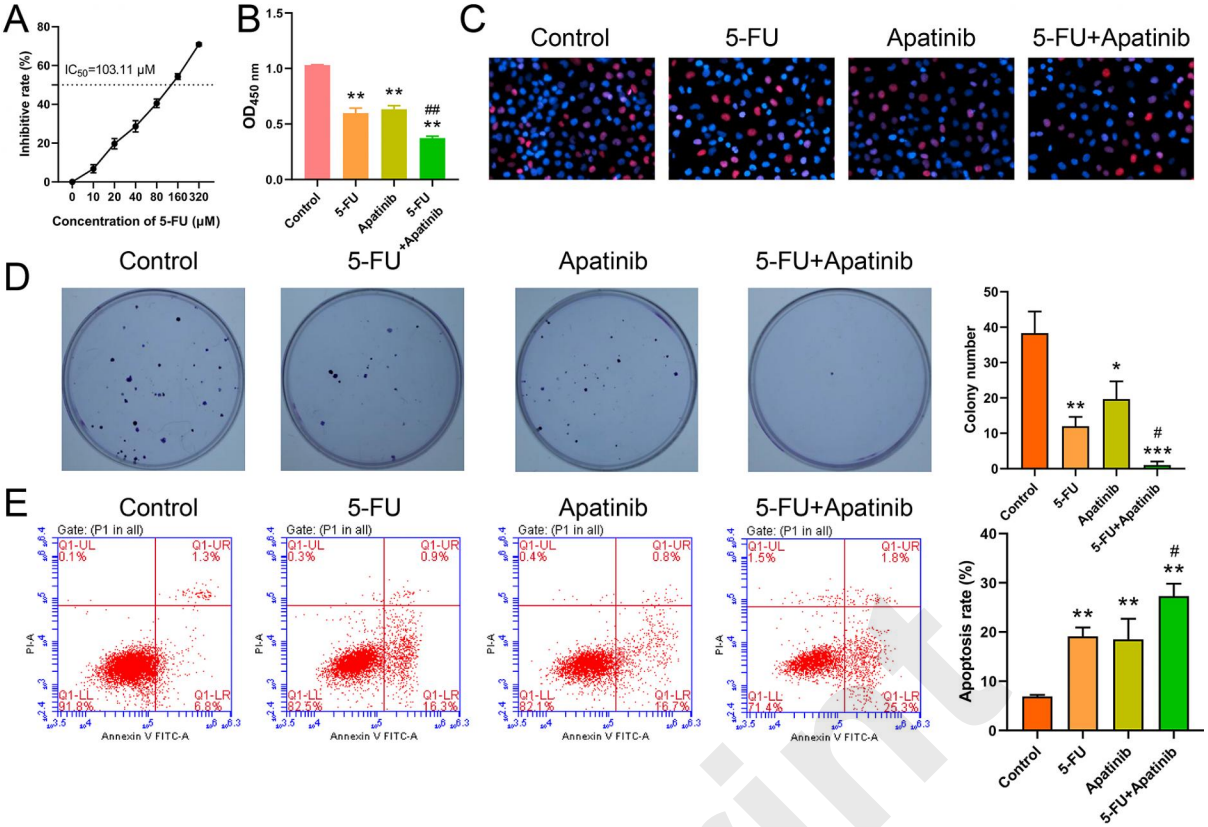
A
Inhibitive rate (%)
IC50=103.11 μM
Concentration of 5-FU (μM)
B
OD450 nm
Control
5-FU
Apatinib
5-FU +Apatinib
C
Control
5-FU
Apatinib
5-FU+Apatinib
D
Control
5-FU
Apatinib
5-FU+Apatinib
Colony number
E
Control
5-FU
Apatinib
5-FU+Apatinib
Gate: (P1 in all)
Annexin V FITC-A
PI-A
Apoptosis rate (%)

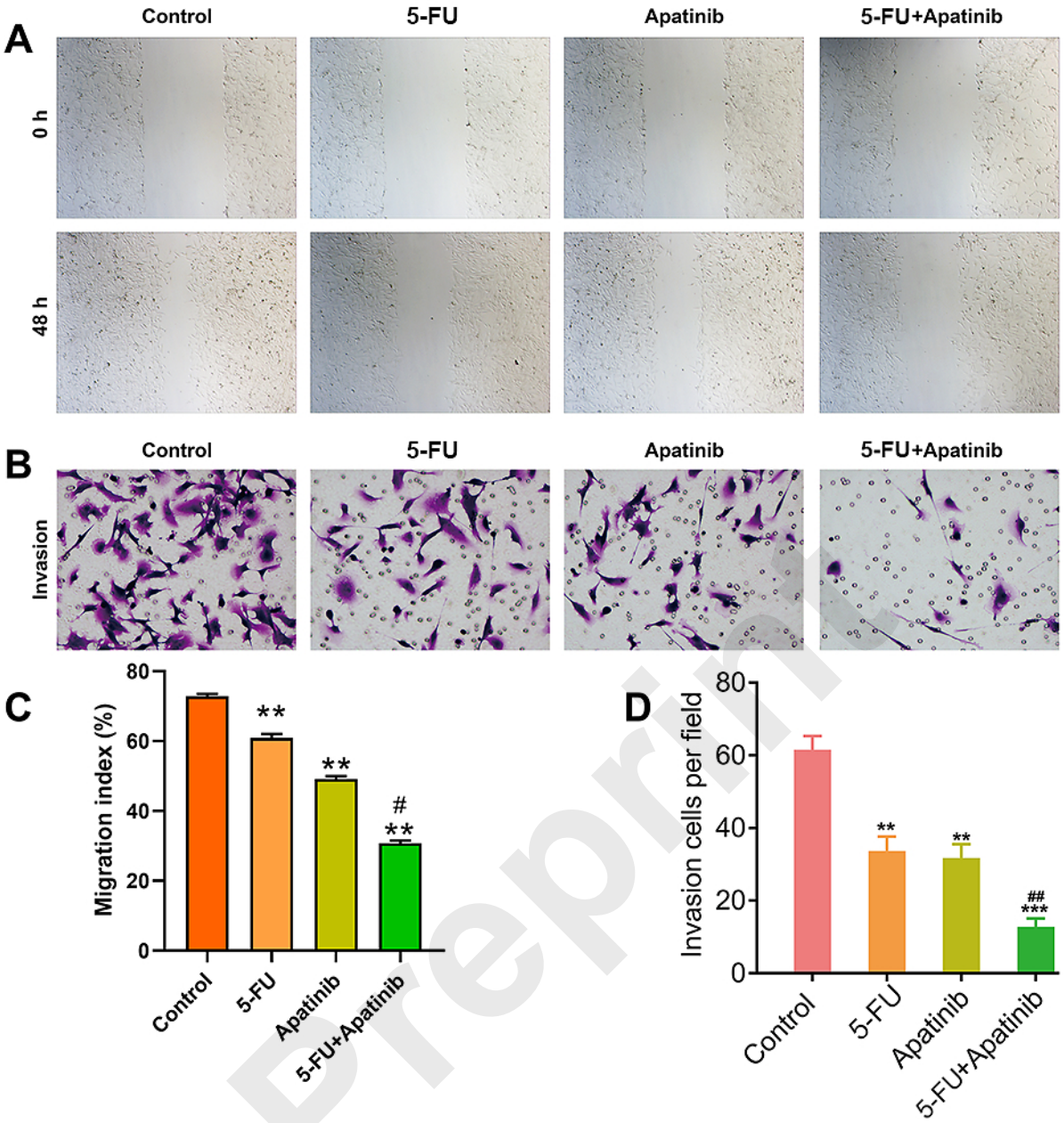
A
Control
5-FU
Apatinib
5-FU+Apatinib
0 h
48 h
B
Control
5-FU
Apatinib
5-FU+Apatinib
Invasion
C
Migration index (%)
80
60
40
20
0
**
**
#
**
Control
5-FU
Apatinib
5-FU+Apatinib
D
Invasion cells per field
80
60
40
20
0
**
**
##
***
Control
5-FU
Apatinib
5-FU+Apatinib

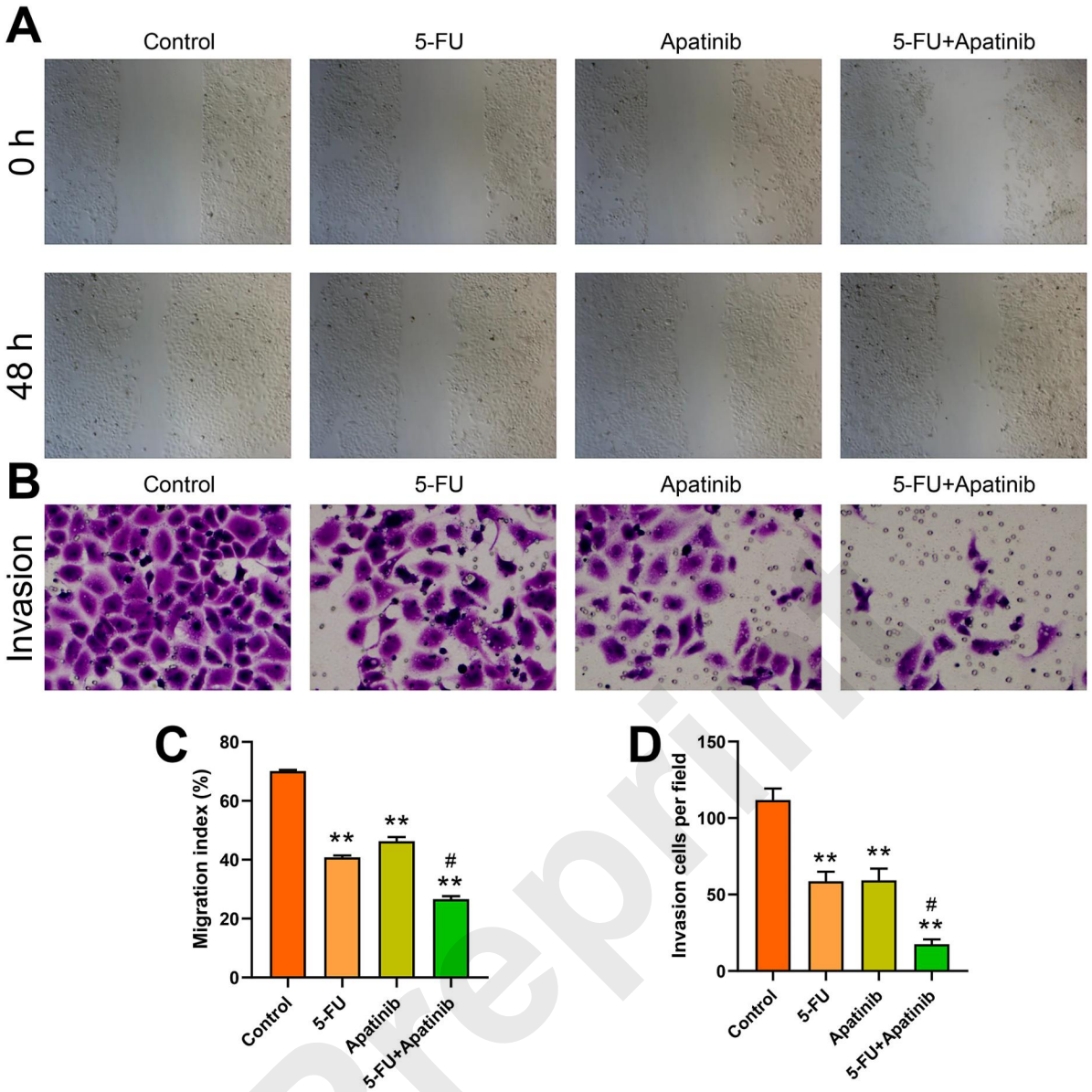
A
Control
5-FU
Apatinib
5-FU+Apatinib
0 h
48 h
B
Control
5-FU
Apatinib
5-FU+Apatinib
Invasion
C
Migration index (%)
80
60
40
20
0
**
**
#
**
Control
5-FU
Apatinib
5-FU+Apatinib
D
Invasion cells per field
150
100
50
0
**
**
#
**
Control
5-FU
Apatinib
5-FU+Apatinib

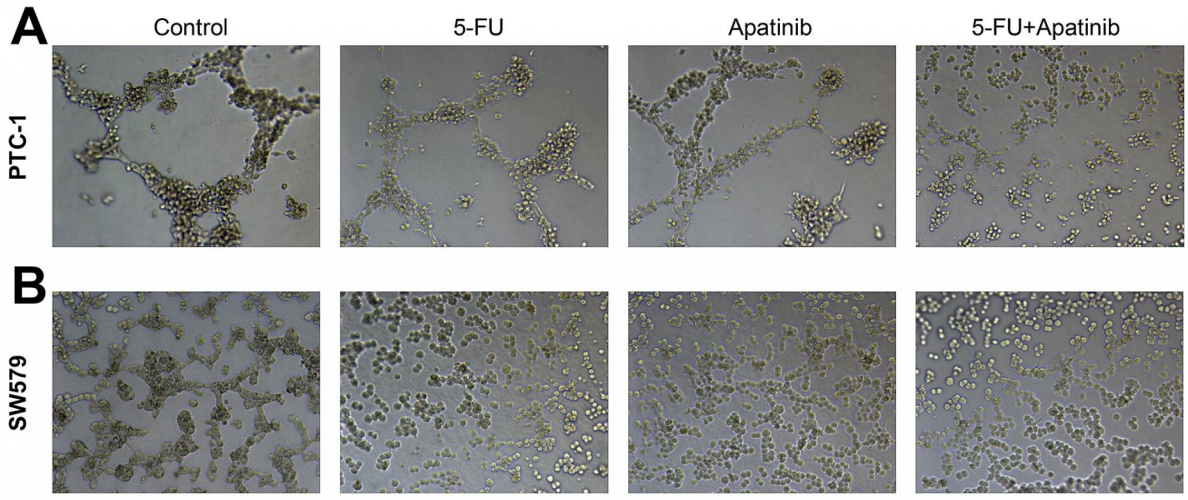

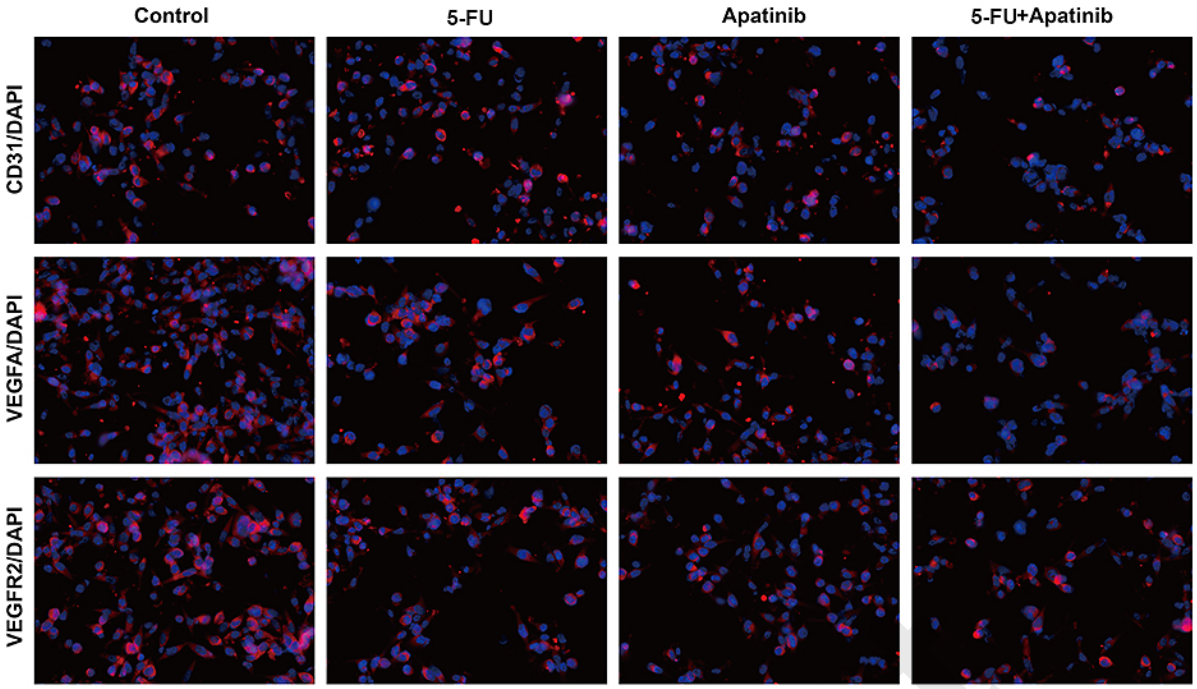
Control
5-FU
Apatinib
5-FU+Apatinib
CD31/DAPI
VEGFA/DAPI
VEGFR2/DAPI

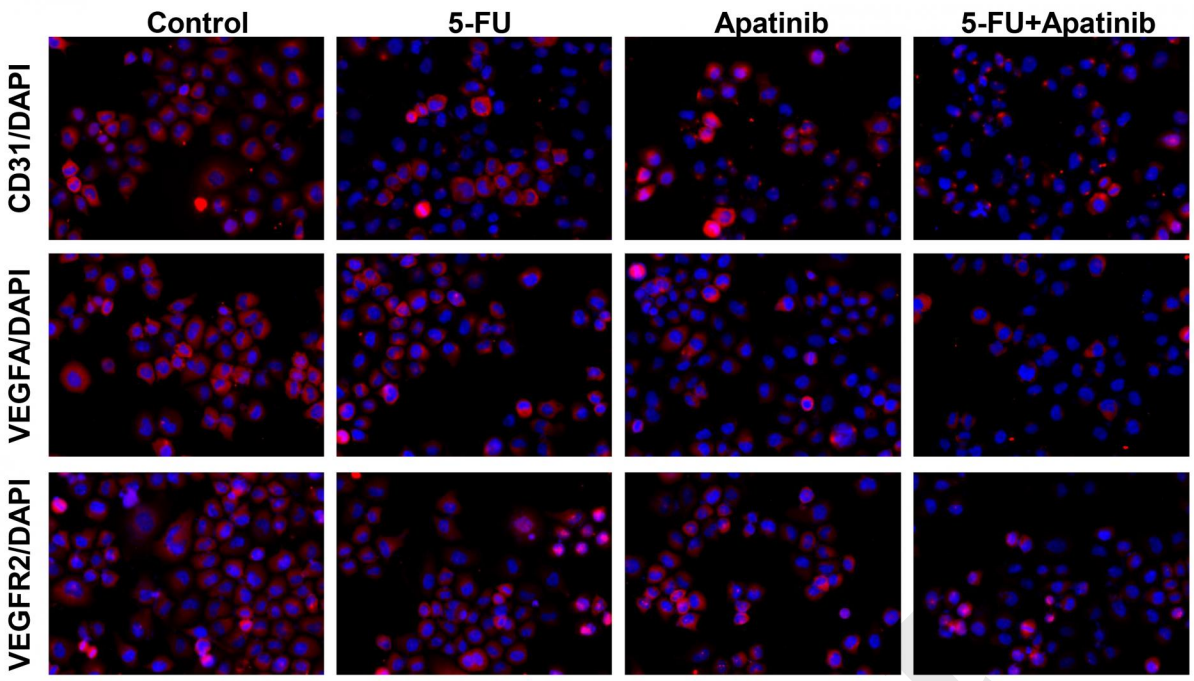
Control
5-FU
Apatinib
5-FU+Apatinib
CD31/DAPI
VEGFA/DAPI
VEGFR2/DAPI

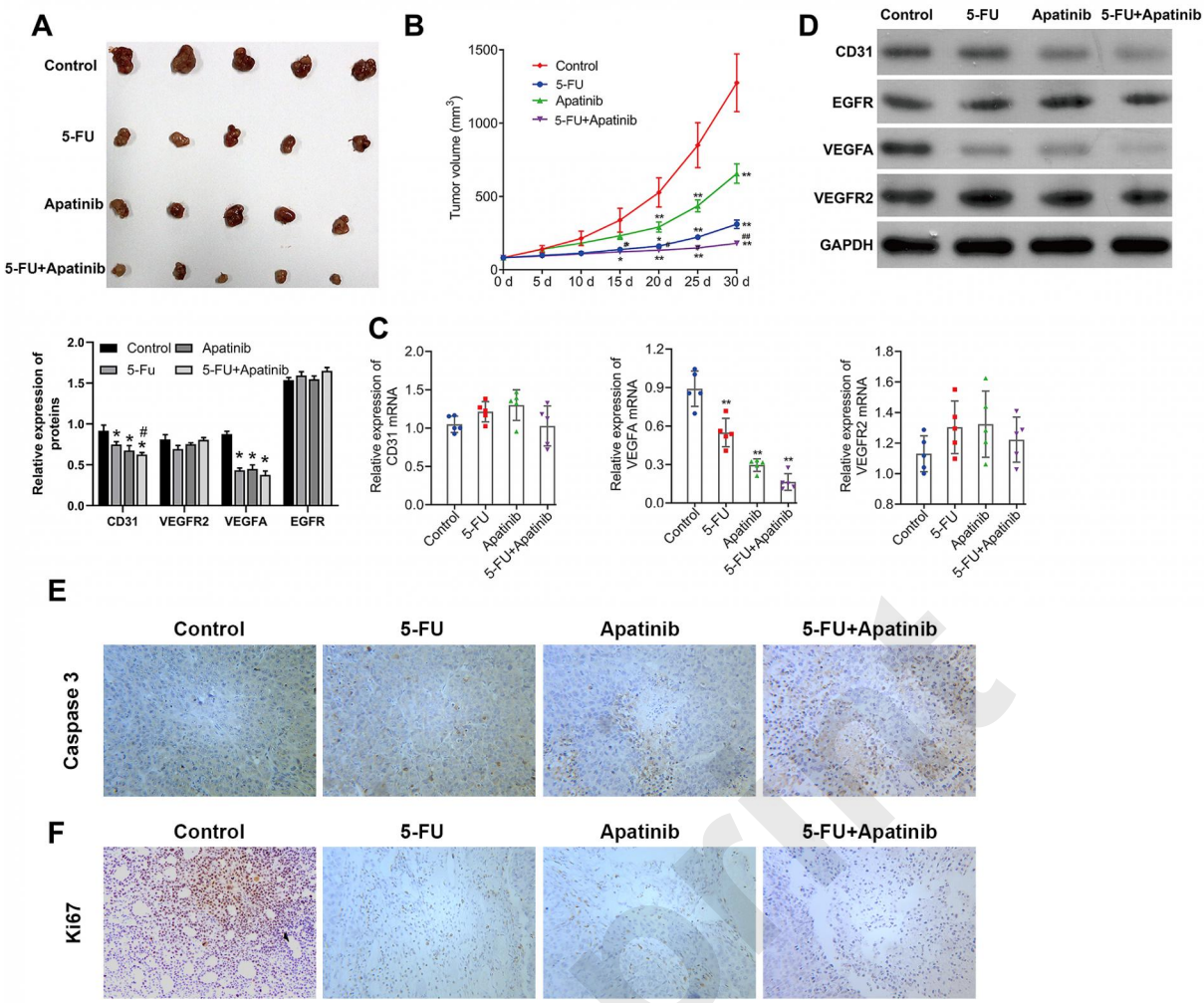
A
Control
5-FU
Apatinib
5-FU+Apatinib
B
Tumor volume (mm3)
1500
1000
500
0
0 d
5 d
10 d
15 d
20 d
25 d
30 d
Control
5-FU
Apatinib
5-FU+Apatinib
D
Control
5-FU
Apatinib
5-FU+Apatinib
CD31
EGFR
VEGFA
VEGFR2
GAPDH
Relative expression of proteins
Control
Apatinib
5-Fu
5-FU+Apatinib
CD31
VEGFR2
VEGFA
EGFR
C
Relative expression of CD31 mRNA
Relative expression of VEGFA mRNA
Relative expression of VEGFR2 mRNA
Control
5-FU
Apatinib
5-FU+Apatinib

E
Control
5-FU
Apatinib
5-FU+Apatinib
Caspase 3
F
Control
5-FU
Apatinib
5-FU+Apatinib
Ki67

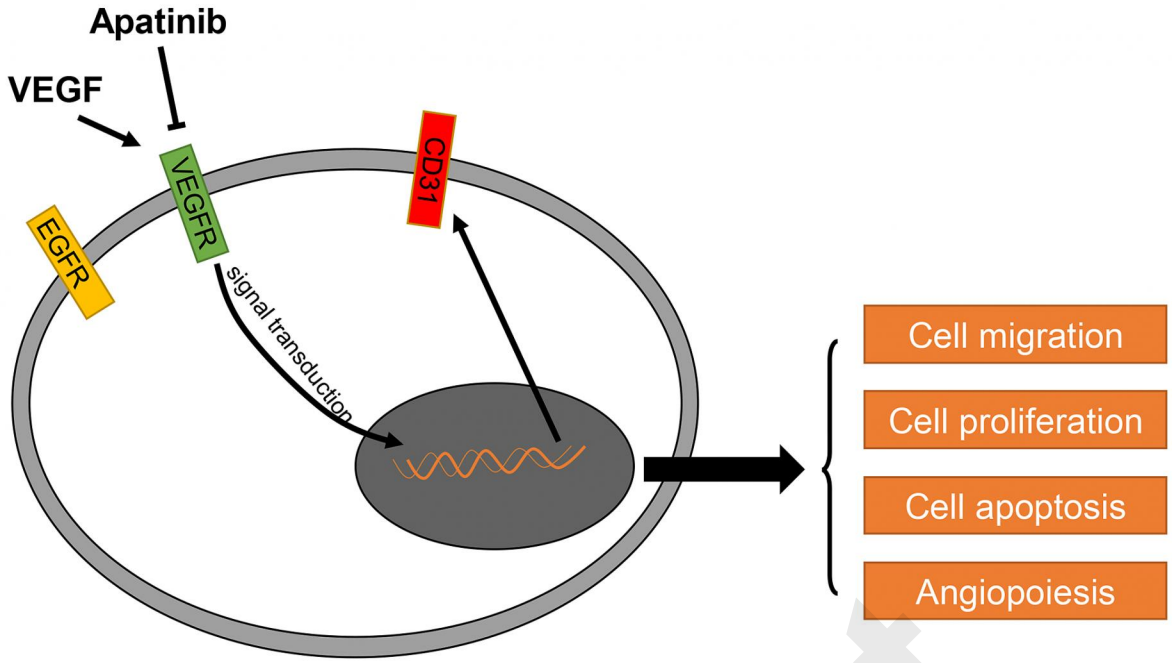
Apatinib
VEGF
VEGFR
EGFR
CD31
signal transduction
Cell migration
Cell proliferation
Cell apoptosis
Angiopoiesis